Synthesis and Characterization of Primary Aluminum Parent Amides and Phosphides

ARTICLE *in* ORGANOMETALLICS · DECEMBER 2013

Impact Factor: 4.13 · DOI: 10.1021/om4010675

5 AUTHORS, INCLUDING:

James C Fettinger
University of California, Davis
437 PUBLICATIONS **10,033** CITATIONS

ORGANOMETALLICS

Article

pubs.acs.org/Organometallics

Synthesis and Characterization of Primary Aluminum Parent Amides and Phosphides

Christopher E. Melton,[†] Jonathan W. Dube,[‡] Paul J. Ragogna,*[,‡] James C. Fettinger,[†] and Philip P. Power*[,†]

[†]Department of Chemistry, University of California, One Shields Avenue, Davis, California 95616, United States

[‡]Department of Chemistry and The Center for Advanced Materials and Biomaterials Research (CAMBR), The University of Western Ontario, London, Ontario N6A 5B7, Canada

Supporting Information

ABSTRACT: The synthesis and characterization of the sterically crowded primary alanes $(Ar^{iPr_4}AlH_2)_2$ (Ar^{iPr_4} = C_6H_3-2,6(C_6H_3-2,6-$^iPr_2$)$_2$) and $(Ar^{iPr_8}AlH_2)_2$ (Ar^{iPr_8} = C_6H-2,6(C_6H_2-2,4,6-$^iPr_6$)$_2$-3,5-$^iPr_2$) are described. They, along with their previously reported less-hindered analogue $(Ar^{Me_6}AlH_2)_2$ (Ar^{Me_6} = C_6H_3-2,6(C_6H_2-2,4,6-Me_3)$_2$), were reacted with ammonia to give the parent amido alanes $\{Ar^xAl(H)NH_2\}_2$ (Ar^x = Ar^{Me_6}, **1**; Ar^{iPr_4}, **2**; Ar^{iPr_8}, **3**), which are the first well-characterized hydride amido derivatives of aluminum and are relatively rare examples of parent aluminum amides. In contrast, the reaction of $(Ar^{Me_6}AlH_2)_2$ with phosphine yielded the structurally unique Al/P cage species $\{(Ar^{Me_6}Al)_3(\mu\text{-}PH_2)_3(\mu\text{-}PH)PH_2\}$ (**4**) as the major product and a smaller amount of $\{(Ar^{Me_6}Al)_4(\mu\text{-}PH_2)_4(\mu\text{-}PH)\}$ (**5**) as a minor product. All compounds were characterized by NMR and IR spectroscopy, while compounds **2**−**5** were also characterized by X-ray crystallography.

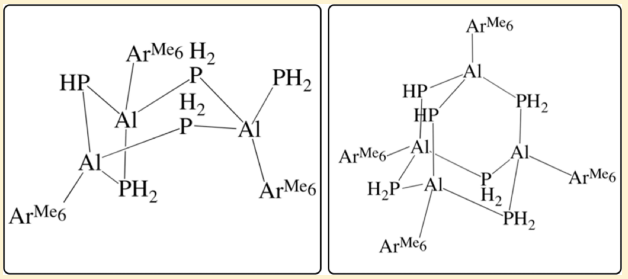

INTRODUCTION

Parent amido (NH_2^-) and parent phosphido (PH_2^-) derivatives of aluminum are relatively rare and little-studied. Only a handful of structurally characterized species are known. These include the aluminum derivatives $\{(Me_3Si)_2AlNH_2\}_2$,[1] $[\{(Me_3Si)_2N\}_2AlNH_2]_2$,[1,2] $Al\{(NH_2)_2Al(SiMe_3)_2\}_3$,[2,3] $Al[(NH_2)_2Al\{N(SiMe_3)_2\}_2]$,[2] and $(R_2AlNH_2)_3$ (R = Me, ^{t}Bu),[4] some of which are illustrated schematically in Figure 1. The parent amides are generally prepared by reaction of ammonia with reactive Al-R moieties (R = $N(SiMe_3)_2$, $SiMe_3$, Me, or ^{t}Bu) as shown in eq 1. However, Roesky and co-workers showed that by using the bulky, bidentate β-diketiminate ligand $HC\{C(CH_3)N(2,6\text{-}^iPr_2C_6H_3)\}_2$, (L), they could prepare the terminal parent amido species $LAl(NH_2)_2$ featuring terminal amido ligands by direct reaction of $LAlCl_2$ with excess ammonia.[5] Amido derivatives of the group 13 metals have been reviewed recently.[6,7]

$$R_3Al + nNH_3 \rightarrow R_{3-n}Al(NH_2)_n + nRH$$
$$R = N(SiMe_3)_2,\ SiMe_3,\ H,\ CH_3,\ C_2H_5$$
$$n = 3,\ 2,\ 1 \qquad (1)$$

The first aluminum parent phosphido complex, $LiAl(PH_2)_4$, was reported by Finholt and co-workers in 1963.[8] Treatment of lithium aluminum hydride, $LiAlH_4$, with PH_3 at low temperature resulted in the formation of a highly pyrophoric, colorless solid with composition $LiAl(PH_2)_4$. Its solid state structure remains unknown, but it has been used as a convenient PH_2^- transfer agent.[9,10] Structures of parent phosphides in which aluminum carries an organic substituent are also relatively scarce. Driess and Monsé reported the preparation of $\{^iBu_2Al(PH_2)\}_n$ from $^iBu_2AlH$ and PH_3.[11] By using low temperature ^1H and ^{31}P NMR spectroscopy, they concluded that the product had a polymeric structure derived from $^iBu_2Al(PH_2)$ monomeric units. Attempts to crystallize the unsolvated compound were unsuccessful, and formation of THF or dimethoxyethane solvates resulted in facile decomposition of the ether donor.

The only structurally characterized parent phosphide derivatives of aluminum are those synthesized by Scheer and co-workers.[12−15] They are derived from the transition metal phosphine complexes $W(CO)_5PH_3$ and $Cr(CO)_5PH_3$. For example, the reaction of $W(CO)_5PH_3$ with $AlH_3(NMe_3)$ afforded the compound $[(CO)_5W]PH_2AlH_2(NMe_3)$ and several related species, generated by further reaction with a Lewis base or thermolysis, as shown in Figure 2.

We now show that the use of bulky terphenyl substituents at aluminum can stabilize both primary amido and phosphido derivatives and show that the reactions of the sterically crowded primary alanes $\{Ar^{Me_6}AlH_2\}_2$ (Ar^{Me_6} = C_6H_3-2,6(C_6H_2-2,4,6-Me_3)$_2$)[16] and the previously unreported bulky alanes $\{Ar^{iPr_4}AlH_2\}_2$ (Ar^{iPr_4} = C_6H_3-2,6-$^iPr_2$)$_2$) and $\{Ar^{iPr_8}AlH_2\}_2$ (Ar^{iPr_8} = C_6H-2,6(C_6H_3-2,4,6-$^iPr_3$)$_2$-3,5-$^iPr_2$) with ammonia to afford the simple bridged dimers $\{Ar^{Me_6}Al(\mu\text{-}NH_2)H\}_2$ (**1**),

Received: November 1, 2013
Published: December 19, 2013

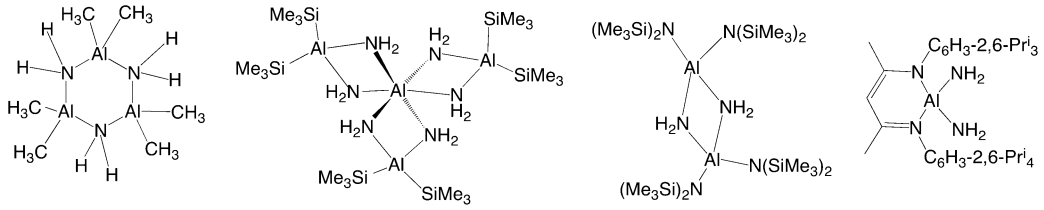

Figure 1. Structurally characterized examples of some parent amido aluminum species.[1−5]

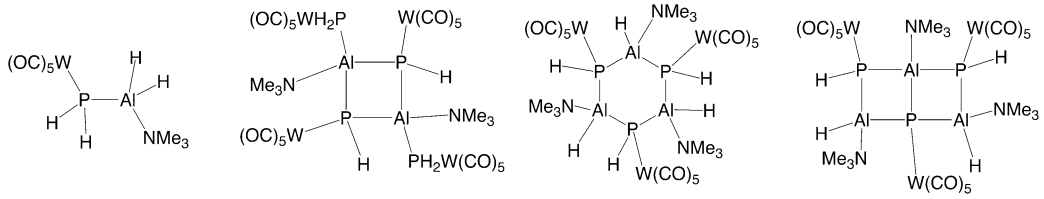

Figure 2. Examples of aluminum parent phosphides.

{Ar^{iPr_4}Al(μ-NH$_2$)H}$_2$ (**2**), and {Ar^{iPr_8}Al(μ-NH$_2$)H}$_2$ (**3**). In contrast, we show that the reaction of {Ar^{Me_6}AlH$_2$}$_2$ with phosphine yields two different complex cage species: (Ar^{Me_6}Al)$_3$(PH$_2$)$_4$(PH) (**4**) and (Ar^{Me_6}Al)$_4$(PH$_2$)$_4$(PH)$_2$ (**5**). The new compounds were characterized by multinuclear NMR spectroscopy and X-ray crystallography.

RESULTS AND DISCUSSION

Synthesis. The reactions of {Ar^{x}AlH$_2$}$_2$ (Ar^x = Ar^{Me_6}, Ar^{iPr_4}, Ar^{iPr_8}) with ammonia were accomplished as in eq 2 at room temperature and approximately atmospheric pressure.

$$[Ar^xAlH_2]_2 + 2NH_3 \rightarrow [Ar^xAlH(NH_2)]_2 + 2H_2$$
$$Ar^x = Ar^{Me_6}, Ar^{iPr_4}, Ar^{iPr_8} \quad (2)$$

Two molar equivalents of dry, deoxygenated ammonia per one stoichiometric equivalent of alane dimer were added to the headspace of a flask containing the solution of the *m*-terphenyl alane in toluene. The reaction was stirred for 18 h at room temperature and then concentrated to yield X-ray quality crystals of the general formula {Ar^{x}Al(H)NH$_2$}$_2$ (Ar^x = Ar^{iPr_4}, Ar^{iPr_8}). Unfortunately, several attempts at crystallization from various solvents did not produce X-ray diffraction-quality crystals of the {Ar^{Me_6}Al(H)NH$_2$}$_2$ derivative (**1**). An interesting aspect of the ^{1}H NMR spectra of **1**−**3** is the appearance of the Al−NH$_2$ hydrogen resonances at higher field than other known parent amides. Previous reports of aluminum parent amides have reported the μ^2-NH$_2$ resonances at ca. 0.75 ppm,[1−4] but in the *m*-terphenyl substituted examples, the μ-NH$_2$ signal is shifted upfield to −0.40 ppm in **1**, −0.65 ppm in **2**, and −0.22 ppm in **3**. The related gallium species, {Ga{C$_6$H$_2$-2,6(C$_6$H$_3$-2,6-^{i}Pr$_2$)-4-SiMe$_3$}(H)NH$_2$}$_2$, displays an NH$_2$ resonance at −0.5 ppm,[17] and the N−H resonance of the LAl(NH$_2$)$_2$ amide was observed at −0.52 ppm.[5] This suggests that the origin of this change is likely due to the magnetic field associated with the induced aromatic ring current of the nearby *m*-terphenyl flanking rings.

Structures similar to **1** and **2** are precedented only by the related gallium species {Ga{C$_6$H$_2$-2,6(C$_6$H$_3$-2,6-^{i}Pr$_2$)-4-SiMe$_3$}-(H)NH$_2$}$_2$,[17] which contains both hydride and parent amido groups attached to a group 13 metal. However, that compound was synthesized by a different route involving the reaction of the Ga(I) digallene terphenyl derivative {Ga{C$_6$H$_2$-2,6(C$_6$H$_3$-2,6-^{i}Pr$_2$)$_2$-4-SiMe$_3$}$_2$ via insertion of the gallium into an N−H bond.[17] As in the case of aluminum, several other gallium parent amido species of formula {R$_2$Ga(NH$_2$)}$_2$ (R = H, Me, Et, CH$_2$^{t}Bu, ^{t}Bu) are also known; however, these also carry two organic substituents at the metal.[18−24]

The reaction of (Ar^{Me_6}AlH$_2$)$_2$ with an excess of phosphine gas (80 psi) for 24 h results in very different products than the reaction with ammonia (Scheme 1). The ^{31}P{^{1}H} NMR spectrum of the reaction mixture features four dominant resonances (δ_P = −265 (td, P$_c$), −258 (td, P$_b$), −201 (td, P$_a$), −182 (tddd, P$_d$)), which integrate to an approximate 1:1:2:1 ratio (Figure 3). The ^{31}P{^{1}H} NMR spectrum was simulated as an A$_2$BCD spin system with all the coupling constants reproducing the peak shapes and heights of the experimental spectrum very well. Determining the P−P coupling constants

Scheme 1. Synthesis of the Phosphides 4 and 5, and a Schematic Illustration of the Phosphorus Labeling

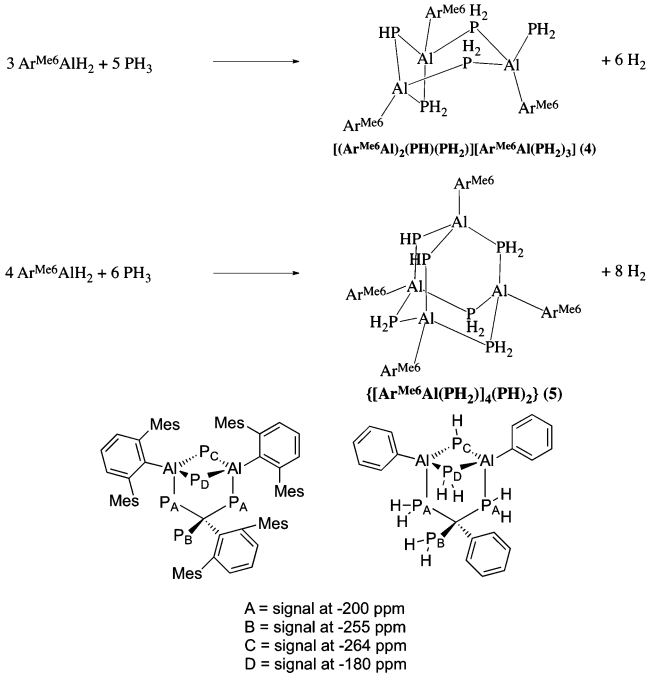

dx.doi.org/10.1021/om4010675 | *Organometallics* 2014, 33, 329−337

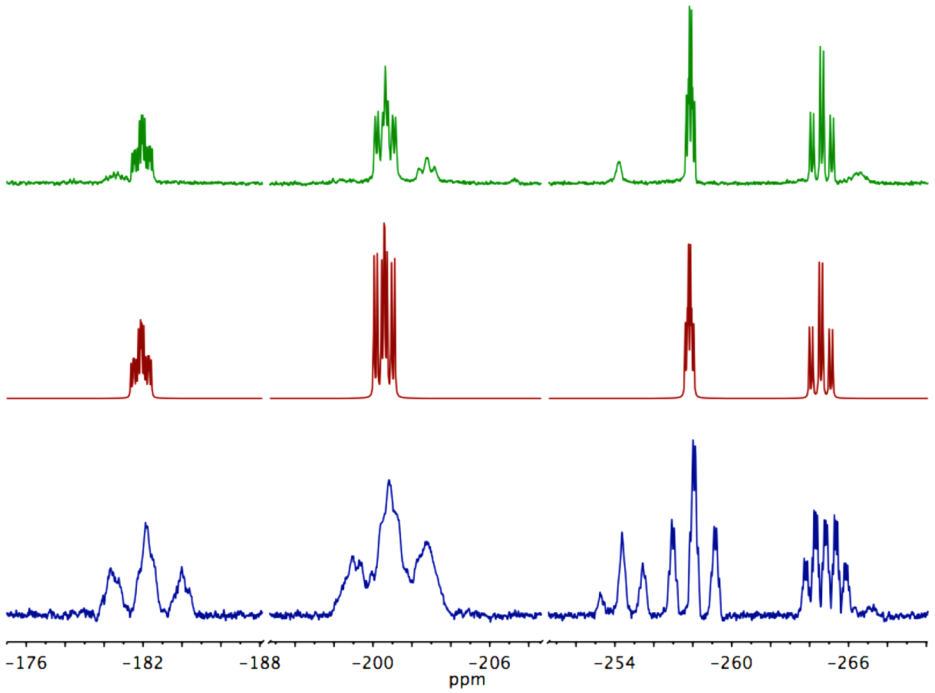

Figure 3. Plots of the $^{31}P\{^{1}H\}$ NMR spectrum of crystallized **4** (top), the simulated $^{31}P\{^{1}H\}$ NMR spectrum of **4** as a A_2BCD spin system (center), and the ^{31}P NMR spectrum of crystallized **4** (bottom). The resonances from left to right in the spectrum correspond to P_d, P_a, P_b, and P_c, respectively. Note the presence of the daughter signals, potentially due to the other geometrical isomer, even after crystallization.

required trial and error in the simulation program, in addition to the normal data analysis on the experimental spectrum ($^{2}J_{Pa-Pb}$ = 26.7 Hz, $^{2}J_{Pa-Pc}$ = 82.5 Hz, $^{2}J_{Pa-Pd}$ = 62.2 Hz, $^{4}J_{Pb-Pd}$ = 17.2 Hz, $^{2}J_{Pc-Pd}$ = 27.5 Hz). A $^{31}P-^{31}P$ COSY experiment showed no observable four bond coupling between P_B and P_C, while all the other phosphorus nuclei couple to one another. This observation was also reproduced in the simulated spectrum. The proton coupled ^{31}P NMR spectrum displays three triplets for P_A, P_B, and P_D indicative of a PH_2 fragment (P_A $^{1}J_{P-H}$ = 299 Hz, P_B $^{1}J_{P-H}$ = 175 Hz, P_D $^{1}J_{P-H}$ = 295 Hz). The resonance for the PH fragment, P_C, appears as a quintet of quintets in a 1:2:2:2:1 ratio because of the overlap of the doublet from the P−H coupling and P−P bond couplings (P_C $^{1}J_{P-H}$ = 168 Hz, $^{2}J_{P-P}$ = 82.5 Hz). Each resonance in the $^{31}P\{^{1}H\}$ NMR spectrum has a related daughter signal of approximately 20% intensity. Crystals suitable for X-ray diffraction studies were obtained from a saturated pentane solution stored at −30 °C, and the $^{31}P\{^{1}H\}$ NMR spectrum still showed the presence of both signals in a comparable ratio, suggesting that the second set of resonances could be a result of an isomer with similar solubility to the major product. The two products are not in equilibrium, as the ratios of these signals do not change over the course of a variable-temperature NMR study. The solid-state structure (schematically drawn in Scheme 1) was determined to be $\{(Ar^{Me_6}Al)_3(\mu\text{-}PH_2)_3(\mu\text{-}PH)(PH_2)\}$ (**4**) by single crystal X-ray diffraction studies (see below), confirming the conclusions drawn from the observed NMR data. From the solid-state structure one can envision that the two isomers observed in solution are where the bridging PH fragment and the terminal PH_2 fragment are cis and trans to one another. The solid-state structure also possesses some disorder in the core ring, which is consistent with the cocrystallization of the cis and trans isomers. The ^{1}H NMR spectrum of **4** reveals a similar trend to that observed for the N−H hydrogens in **1**−**3**, with the hydrogens bound to phosphorus shifted upfield relative to what is usually observed in phosphorus (δ_H = −1.16 (dt), −0.22 (dt)). Broad resonances adjacent to the hydride signals are also observed and possess an integration ratio similar to the isomer identified in the $^{31}P\{^{1}H\}$ NMR spectrum. In addition to the isomer of **4**, another product (compound **5**) of significantly lower yield (ca. 2% by $^{31}P\{^{1}H\}$ NMR spectroscopy) was identified in the $^{31}P\{^{1}H\}$ NMR spectrum (Figure S8, in the Supporting Information) and crystallographically characterized. Unfortunately, attempts to isolate usable quantities of **5** were unsuccessful, as it cocrystallizes with compound **4**. It should be noted that altering the reaction conditions did not change the ratios of the products observed, so that compound **5** is always obtained in minor quantities. Compound **4** is highly soluble in aliphatic and aromatic hydrocarbon solvents alike and is stable indefinitely in the solid state at room temperature under a nitrogen atmosphere. This compound is not stable in solution at elevated temperatures (ca. 70 °C), and decomposition products and hydrogen gas are observed in both the $^{31}P\{^{1}H\}$ and ^{1}H NMR spectra after three hours of heating.

Well-characterized crystalline products resulting from the addition of phosphine to aluminum hydrides appear to be unknown. However, the original work of Coates and Beachley[25,26] and their co-workers showed that the organophosphido species $(Me_2MEMe_2)_3$ (M = Ga or In; E = P or As) could be obtained from the reaction of dimethyl phosphine or arsine with trimethyl gallium or indium. In addition, Cowley, Jones, and co-workers showed that the trimers $\{^{t}BuGa(EH_2)\}_3$ (E = P or As) were obtainable from the reaction of phosphine or arsine with $Ga^{t}Bu_3$.[27] More recently, Robinson and his group showed that the reaction of the terphenyl gallium halide $GaCl_2Ar^{iPr_6}$ (Ar^{iPr_6} = C_6H_3-2,6(C_6H_2-2,4,6-$^{i}Pr_3$)$_2$) with P(SiMe$_3$)$_3$ yielded the unusual trimetallic species $Ar^{iPr_6}Ga(\mu\text{-}GaH)(\mu\text{-}PH_2)_2GaAr^{iPr_6}$, in which the outer two Ar^{iPr_6} substituted galliums of the metal−metal bonded trigallium

dx.doi.org/10.1021/om4010675 | *Organometallics* 2014, 33, 329−337

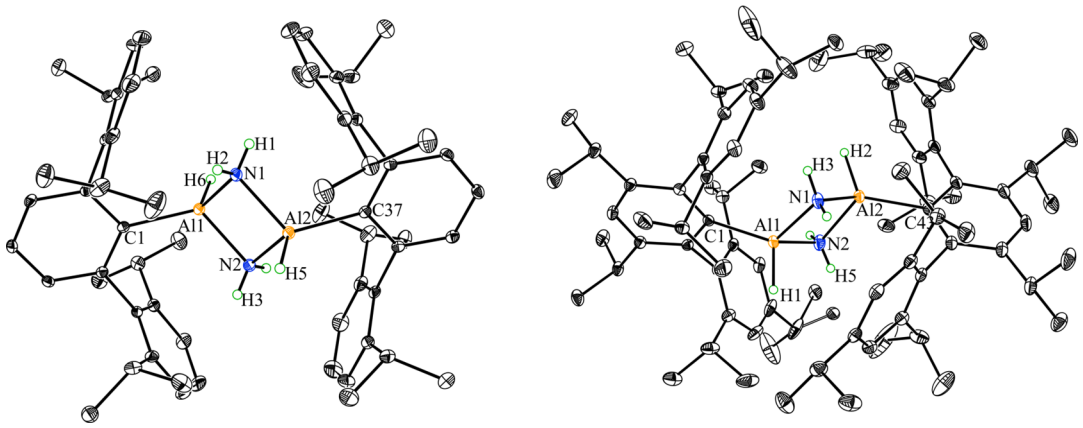

Figure 4. Thermal ellipsoid plots of **2** and **3** at the 30% probability level. Hydrogens bonded to carbon and the cocrystallized solvent molecules are not shown for clarity.

moiety $Ar^{iPr_6}Ga(GaH)GaAr^{iPr_6}$ are bridged by two parent phosphide PH_2 ligands. A variety of mechanisms were proposed to account for the gallium ligand stripping.[28]

The origin of the complex structures of **4** and **5** is presently unclear. The elimination of PH_3 from metal parent phosphides has been observed in pyrolysis studies of $Ca(PH_2)_2$[29] and $M(PH_2)_3$ (M = Eu, Yb)[30,31] as well as in the room temperature formation of $[^iPr_2NBPH]_3$.[33] The observation of PH_3 production during pyrolysis of inorganic metal phosphides suggests that the mechanism should be based on the protonation of PH_2^- groups and subsequent dissociation of the resulting PH_3 ligand. Indeed, the structural characterizations of $[^iPr_2NBPH]_2$ and its $Cr(CO)_5$-trapped intermediate $^iPr_2NB[PH_2Cr(CO)_5]_2$[33] by Nöth, Paine, and co-workers strongly suggest that this is the case. The variety of compounds that release PH_3 by this mechanism could suggest that the protonation−dissociation transformation is also in effect for our aluminum system. The distinct coordination geometries of Al1/Al2 and Al3 suggest that the molecule may be thought of as being composed of the complex ions $[(Ar^{Me_6}Al)_2(\mu\text{-}PH_2)(\mu\text{-}PH)]^{1+}$ and $[Ar^{Me_6}Al(PH_2)_3]^{1-}$. The cation $[(Ar^{Me_6}Al)_2(\mu\text{-}PH_2)(\mu\text{-}PH)]^{1+}$ is similar to Nöth and Paine's borylphosphide $[^iPr_2NBPH]_2$ because of their 4-membered ring structures and their monosubstitution by organic ligands. It should also be noted that deprotonation of the PH_2^- ligand gives the aluminum congener of $[^iPr_2NBPH]_2$. These similarities suggest that this segment of the molecule is formed by the protonation−dissociation mechanism, which Paine suggested was in effect for $[^iPr_2NBPH]_2$. The four-coordinate aluminum atom and terminally bound phosphides of $[Ar^{Me_6}Al(PH_2)_3]^{1-}$ suggest that this entity could also arise from deprotonation of PH_3 by $[Ar^{Me_6}AlH_2]_2$. While this literature precedent provides a logical starting point for a description of a possible mechanism, we presently have no evidence supporting or refuting such reactivity. Therefore, any further discussion of a mechanistic proposal for the formation of these complex architectures would be premature at this stage and will be a topic of our future studies with these compounds.

Solid-State Structures. The thermal ellipsoid plots of the products $\{Ar^{iPr_4}AlH(NH_2)\}_2$ (**2**) and $\{Ar^{iPr_8}AlH(NH_2)\}_2$ (**3**) are shown in Figure 4. Selected bond lengths and angles are given in Table 1. Both products crystallized as dimeric species in which the aluminum atoms are bridged essentially symmetrically by two $-NH_2$ groups. The hydrides are bound in terminal fashion and the *m*-terphenyl ligands are disposed in a trans orientation with respect to an essentially planar Al_2N_2 core. The Al−N bond lengths in **2** average 1.912(4) Å, and those in **3** average 1.936(3) Å. The internal Al_2N_2 ring angles at aluminum and nitrogen average 86.79(2) and 93.22(14)° in **2**, and 86.6(4) and 93.5(2)° in **3**. The slightly longer Al−N distances in the more crowded **3** are also mirrored in the Al−C bond lengths, which are slightly longer in **3** (avg. 2.002(8) Å) than they are in **2** (1.981(1) Å). The Al1−Al2 separations in **2** and **3** are 2.7790(8) and 2.8194(6) Å, respectively. The longer distance in **3** is also consistent with the greater crowding due to the larger size of the Ar^{iPr_8} substituent.

Table 1. Selected Bond Distances (Å) and Angles (°) for 2 and 3

2		3	
Al1−N1	1.9103(14)	Al1−N1	1.9322(14)
Al1−N2	1.9145(15)	Al1−N2	1.9425(13)
Al1−C1	1.9807(16)	Al1−C1	2.0106(14)
Al1−H1	1.52(2)	Al1−H1	1.54(2)
Al2−N1	1.9096(15)	Al2−N1	1.9333(14)
Al2−N2	1.9141(14)	Al2−N2	1.9358(16)
Al2−C37	1.9806(15)	Al2−C43	1.9931(14)
Al2−H2	1.51(2)	Al2−H2	1.50(2)
N1−Al1−N2	86.77(6)	N1−Al1−N2	85.97(6)
N1−Al2−N2	86.80(6)	N1−Al2−N2	86.13(6)
Al1−N1−Al2	93.36(6)	Al1−N1−Al2	93.67(6)
Al1−N2−Al2	93.08(6)	Al1−N2−Al2	93.28(5)
N1−Al1−C1	115.98(7)	N1−Al1−C1	119.40(6)
N2−Al1−C1	117.26(7)	N2−Al1−C1	121.27(6)
N1−Al1−H1	110.3(7)	N1−Al1−H1	103.1(6)
N2−Al1−H1	108.2(7)	N2−Al1−H1	103.8(6)

The sums of the angles between the amido and aryl substituents at the aluminum atoms in **3** are also wider than those in **2** (cf. 326.64(7) in **3**, versus 320.01(7) in **2**. The Al−N distances resemble those in the previously reported aluminum parent amides $\{(Me_3Si)_2AlNH_2\}_2$,[1] $[\{(Me_3Si)_2N\}_2AlNH_2]$,[2] and $(Me_2AlNH_2)_3$,[4] which feature Al−N distances that vary from ca. 1.92 to 1.96 Å. The Al−N distances in **1** and **2** are shorter than the average Ga−N distance (1.987(2) Å) of those in the gallium dimer $[Ga\{C_6H_2\text{-}2,6(C_6H_3\text{-}2,6\text{-}^iPr_2)_2\text{-}4\text{-}SiMe_3\}(H)NH_2]_2$,[17] despite the smaller radius of gallium.[33] This is partly a result of the higher ionic character of the Al−N bond in comparison to that of Ga−N.[34] The Al−C bond lengths are

dx.doi.org/10.1021/om4010675 | *Organometallics* 2014, 33, 329−337

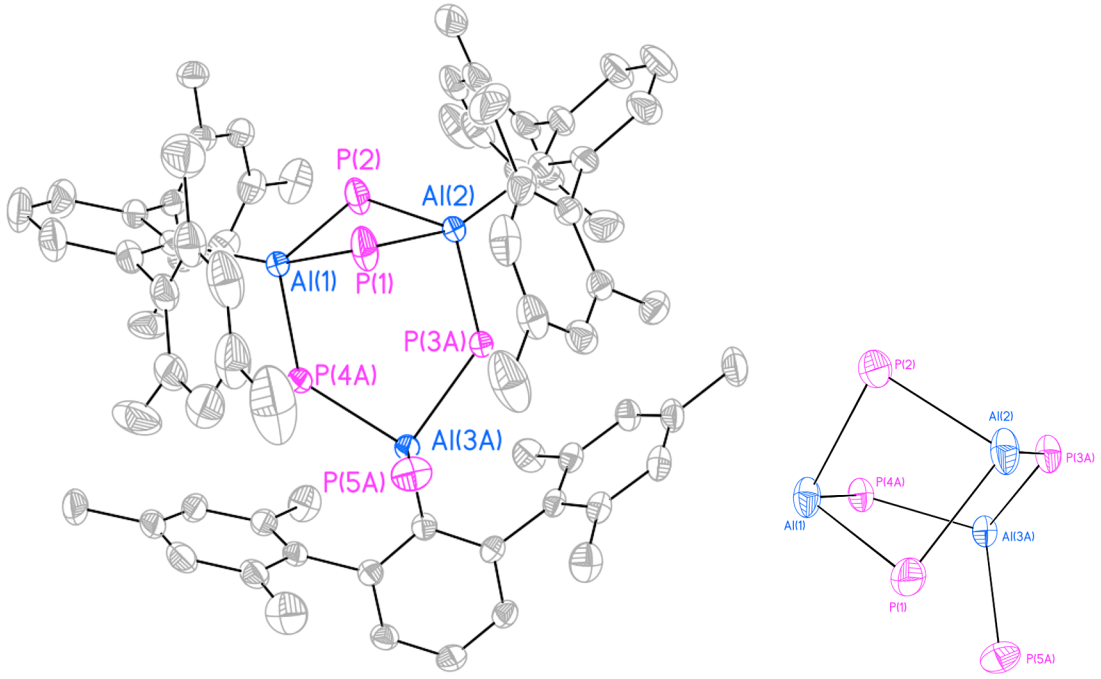

Figure 5. Thermal ellipsoid plot of **4** at 30% probability (left; hydrogen atoms are not shown for clarity) and the Al_3P_5 core (right). Bond lengths and angles are given in Table 2

Table 2. Selected Bond Lengths (Å) and Angles (°) for 4 and 5

4		5			
Al1−P1	2.3687(14)	Al1−P1	2.4603(15)	Al4−P4	2.4246(14)
Al1−P2	2.3681(14)	Al1−P2	2.3143(14)	Al4−P6	2.3239(14)
Al1−P4A	2.4781(19)	Al1−P3	2.4502(13)	Al4−C73	2.016(3)
Al1−C1	1.990(3)	Al1−C1	2.013(3)	P1−H1PA	1.34(4)
Al2−P1	2.3704(15)	Al2−P2	2.3170(14)	P1−H1PB	1.33(4)
Al2−P2	2.3531(15)	Al2−P4	2.4312(15)	P2−H2PA	1.45(3)
Al2−P3A	2.4552(19)	Al2−P5	2.4401(13)	P3−H3PA	1.37(4)
Al2−C25	1.986(3)	Al2−C25	2.013(3)	P3−H3PB	1.33(4)
Al3A−P3A	2.409(2)	Al3−P3	2.4348(14)	P4−H4PA	1.30(3)
Al3A−P4A	2.416(2)	Al3−P5	2.4524(13)	P4−H4PB	1.39(3)
Al3A−P5A	2.378(2)	Al3−P6	2.3239(15)	P5−H5PA	1.35(4)
Al3A−C49	1.977(3)	Al3−C49	2.027(3)	P5−H5PB	1.58(4)
		Al4−P1	2.4504(14)	P6−H6PA	1.45(4)
P1−Al1−P2	85.80(4)	P1−Al1−P3	93.02(5)		
Al1−P1−Al2	88.67(5)	P3−Al3−P5	91.72(4)		
P2−Al2−P1	86.10(4)	P5−Al2−P4	95.23(5)		
Al1−P2−Al2	89.09(4)	P4−Al4−P1	95.94(4)		
P1−Al1−P4A	108.70(7)	P1−Al1−P2	105.22(5)		
P2−Al2−P3A	99.34(7)	P2−Al2−P5	109.29(5)		
P1−Al2−P3A	108.64(7)	P5−Al3−P6	107.06(5)		
P2−Al2−P4A	98.19(6)	P4−Al4−P6	108.95(5)		
P3A−Al3A−P5A	103.68(9)	C1−Al1−P2	110.32(10)		
P4A−Al3A−P5A	105.39(9)	C25−Al2−P4	109.03(11)		
Al3A−P3A−Al2	120.59(9)	C49−Al3−P6	109.81(10)		
Al3A−P4A−Al1	120.04(8)	C73−Al4−P4	117.38(10)		

similar to those found in other *m*-terphenyl aluminum compounds.[16,35] The *m*-terphenyl ligands are disposed in a trans fashion on each side of the Al_2N_2 plane, as shown by the ipso-C−Al−Al angles, C1−Al1−Al2 138.6(4)° and C43−Al2−Al1 128.9(3)° in **3**, as well as C1−Al1−Al2 128.01(6)° and C31−Al2−Al1 128.25(6)° in **2**. These resemble the corresponding angles in the related gallium species reported earlier by this group, in which the analogous angles are approximately 128°.[24] The hydrogen atoms bound to aluminum were located in the electron density maps for **2** and **3**, and were refined freely. Signals due to the hydrides were observed in the ^{1}H NMR spectra of $\{Ar^{Me_6}Al(H)NH_2\}_2$ and $\{Ar^{iPr_4}Al(H)NH_2\}_2$ as broad absorptions with chemical shifts close to that of the alane starting materials $(Ar^{iPr_8}AlH_2)_2$ and $(Ar^{iPr_4}AlH_2)_2$ (see above).

dx.doi.org/10.1021/om4010675 | *Organometallics* 2014, 33, 329−337

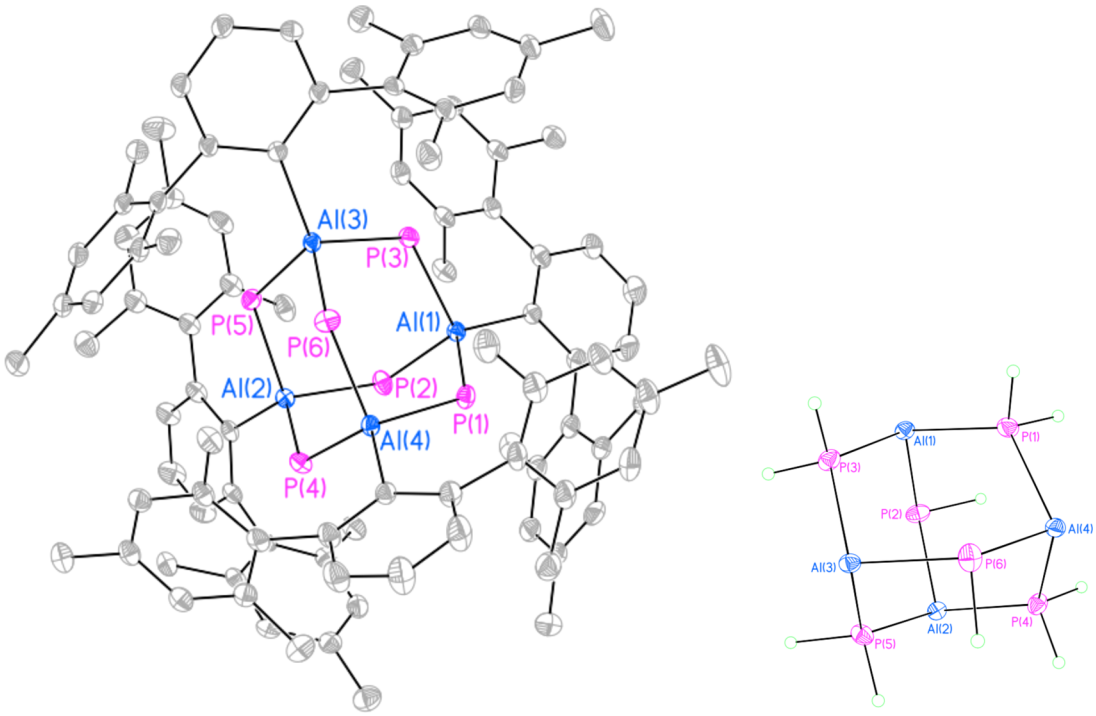

Figure 6. Thermal ellipsoid plot of the minor product **5** at 30% probability (left; hydrogen atoms and toluene solvate molecules are not shown for clarity) and the Al_4P_6 core (right). Bond lengths and angles are given in Table 2

In the ^{1}H NMR spectrum of $\{Ar^{iPr_8}Al(H)NH_2\}_2$, the hydride signal is obscured by the isopropyl methine absorbances, but its presence can be deduced from the integration values of the signals.

The solid state structure of the major Al−P product $\{(Ar^{Me_6}Al)_3(\mu\text{-}PH_2)_3(\mu\text{-}PH)(PH_2)\}$ (**4**) is depicted in Figure 5 with selected metrical parameters listed in Table 2. The compound features three Ar^{Me_6}-substituted aluminum units, three bridging phosphido groups, and a bridging phosphinidido group arranged in a bicyclic fashion. All the aluminums are four-coordinate with no Al−H bonds, in contrast to the products obtained from the activation of ammonia (**1**−**3**). Al3 is unique in that it also carries a terminal phosphido ligand, whereas Al1 and Al2 occupy bridgehead positions in the bicyclic ring system. Al1 and Al2 are linked to each other by PH_2 and PH bridges, and to Al3 by PH_2 bridges. The Al−P bond lengths can be rationalized in terms of the coordination numbers of the phosphorus atoms. Similar to the Al−P bond lengths observed by Scheer,[12−15] which ranged from ca. 2.37 to 2.43 Å, the Al−P distances in **4** range from ca. 2.35 to 2.48 Å. The distances are also similar to those observed in the six-membered ring compounds $[(Me_3Si)_2Al\{P(R)(R^1)\}]_3$ (R(R^1) = Ph(Ph), C_6H_{11}(H)$SiMe_3$($SiMe_3$) (average 2.44 Å),[36] $(Me_2AlPMe_2)_3$ (2.43 Å), or the eight-membered ring species $(Me_2Al)_4\{C_6H_4\text{-}1,2(PH)_2\}$ (2.44 Å).[37] The Al1Al2P1P2 moiety has a butterfly structure with folding along the Al1−Al2 axis. The coordination environment of Al3 is distinct and is formed from two bridging phosphides, a terminal phosphide, and the terphenyl group. The six-membered ring defined by Al1, Al2, Al3, and P1, P3A, and P4A can be thought of as having a "boat" conformation, whereas a second ring, defined by Al1, Al2, Al3, and P2, P3A, and P4A has a "chair" conformation. The angles at Al3, which range from 92° to 121°, are consistent with a distorted tetrahedral coordination. Two isomeric forms of the molecule were observed in the solid state, with the one with an occupation factor of approximately 60% shown in Figure 5 (See Figure S11 in the Supporting Information for a full diagram). In this case, it can be seen that the terminal phosphido phosphorus P5A is in cis orientation with respect to P1, whereas in the second isomer, the terminal phosphido group P5B is arranged cis to P2. Most hydrogen atoms could be located; however, some did not consistently refine to suitable angles and distances because of the inherent ring disorder and the large quantity of disordered solvent molecules. Therefore the phosphorus hydrides have not been included in the refinement; however, their location has been unequivocally proven by NMR spectroscopy. The observed Al−P distances of Al3 are similar to those seen in the Al2P2 ring, each being approximately 2.4 Å long. The interligand angles are distorted from ideal tetragonal angles because of the bulky *m*-terphenyl substituent, which effects a narrowing of P3A−Al3A−P4A angle to 92.73(8)° and widening of the C49−Al3A−P5A angle, 116.76(12)°. In the minor isomer, these angles are similar at 93.03(12)° and 120.34(14)°, respectively.

The solid-state structure for **5** has an adamantane-like core with four aluminum atoms and six bridging phosphorus atoms (Figure 6). The Al−PH_2 bond lengths lie between 2.42−2.47 Å, while the Al−PH bond lengths are shorter, in the range of 2.3143(14) and 2.3239(14) Å. The P−H bond lengths of the PH_2 moiety all lie in the range of 1.30(4)−1.40(4) Å with the exception of one outlier that did not refine suitably. The P−H bond lengths of the PH atoms are both longer at 1.45(4) Å. However, it should be stated that almost all the P−H bond lengths lie within 3σ of each other. The interligand angles around the aluminum atoms are close to tetrahedral, with the exception of four angles, which form the peripheral eight-membered ring (P1−Al1−P3−Al3−P5−Al2−P4−Al4), which range from 91° to 96°. This phenomenon is not observed in

dx.doi.org/10.1021/om4010675 | *Organometallics* 2014, 33, 329−337

admantane itself,[38] but such distortion is seen in several main group analogues of $[(Ar^{Me_6}Al)_4(\mu\text{-}PH_2)_4(\mu\text{-}PH)_2]$.[39−43]

CONCLUSIONS

It has been shown that bulky terphenyl substituents can stabilize parent amido and phosphido derivatives of primary alanes. The products were obtained by treatment of primary alane with either ammonia or phosphine. The results show that while the *m*-terphenyl substituted aluminum hydrido amides are stable species, they display no tendency to release a second equivalent of H_2 and form the aluminum parent imide under the conditions employed. The reactions of a primary alane with PH_3 have also established that the formation of parent aluminum phosphides is possible using the bulky *m*-terphenyl ligands. Unlike the nitrogen analogues, the parent phosphide can release both hydride equivalents to afford PH^{2-} functionalities, which then undergo multiple condensations to form the unique cluster compounds $\{(Ar^{Me_6}Al)_3(\mu\text{-}PH_2)_3(\mu\text{-}PH)(PH_2)\}$ (**4**) and $[(Ar^{Me_6}Al)_4(\mu\text{-}PH_2)_4(\mu\text{-}PH)_2]$ (**5**) with loss of PH_3.

EXPERIMENTAL SECTION

General Methods. All manipulations were carried out under anaerobic and anhydrous conditions using modified Schlenk techniques under an atmosphere of N_2 or in a Vacuum Atmospheres HE-43 drybox. Manipulations for the phosphorus compounds were performed in a MBraun Labmaster 130 drybox. Solvents were dried over an alumina column using the method of Grubbs[44] and were stored over potassium mirrors. $(Ar^{Me_6}AlH_2)_2$,[16] $AlH_3{\cdot}NMe_3$,[45] $(LiAr^{iPr_4})_2$,[46] and $Ar^{iPr_8}Li(Et_2O)$[47] were prepared by literature procedures. Ammonia was dried by dissolving sodium in liquid ammonia to give a blue solution, from which the dry ammonia was then distilled. Phosphine was obtained from Cytec Industries and loaded to the stainless steel Parr reactor via a stainless steel gas line fit with a corrosive gas regulator, purchased from Praxair. ^1H, $^{13}C\{^1H\}$, $^{31}P\{^1H\}$ NMR spectra were recorded either on a Varian Mercury 300 MHz, a Varian INOVA 400 MHz, or a Varian 600 MHz instrument. Infrared spectra were recorded using attenuated total reflectance (ATR) on a Bruker Tensor 27 infrared spectrometer or a Perkin-Elmer PE-1430 spectrometer as Nujol mulls between KBr plates. Melting points were measured in glass capillaries sealed under N_2 by using a Mel-Temp II apparatus and are uncorrected. Note: Phosphine is highly toxic and should be handled with extreme care. The phosphine was handled by at least two personnel equipped with phosphine gas monitors. A stainless steel manifold was used to transfer the gas to the Parr reactor and was disposed of by incineration.

$Li(OEt_2)H_3AlAr^{iPr_4}$. A solution of $AlH_3{\cdot}NMe_3$ (0.971 g, 10.9 mmol) in Et_2O (30 mL) was added dropwise to a stirred slurry of $(LiAr^{iPr_4})_2$ (4.13g, 10.2 mmol) in hexane (30 mL), with cooling to ca. 0 °C. The slurry immediately dissolved upon addition of a few drops of alane solution. Once the addition was complete, the ice bath was removed, and the colorless solution was stirred for a further 18 h at room temperature. The reaction was concentrated under reduced pressure to produce a colorless oil, which could not be induced to crystallize or distill. However, ^1H NMR spectroscopy displayed only signals due to the $Li(OEt_2)H_3AlAr^{iPr_4}$ product. This product was used without further purification. Yield: 4.0 g (90%). ^1H NMR (500 MHz, C_6D_6, 25 °C): δ 7.224−7.139 (m, 4H *m,p*-$H_3C_6R_2$), 3.17 (q, 4H OCH_2CH_3, $^3J_{HH}$ = 6.9 Hz), 3.06 (sept, 4H $CH(CH_3)_2$ $^3J_{HH}$ = 6.9 Hz), 2.29 (bs, 3H AlH_3) 1.298 (d, 12H *J* = 6.9 Hz) 1.12 (d, 12H *J* = 6.9 Hz) 0,966 (d, 6H *J* = 6.9 Hz). FTIR: 1800 m, 1650 br,m. ^{13}C NMR (75 MHz, C_6D_6, 25 °C): δ 146.92, 141.26, 139.75, 131.49, 128.46, 128.28, 128.08, 127.89, 128.05, 123.35, 122.91, 47.90, 31.36, 30.81, 25.09, 24.39, 23.68. FTIR: 1800 m, 1650 br,m. mp 114 °C (with decomposition).

$(Ar^{iPr_4}AlH_2)_2$. $Li(OEt_2)H_3AlAr^{iPr_4}$ (3.60 g, 8.28 mmol) was dissolved in 50% Et_2O/hexane (50 mL) and cooled to ca. −10 °C in a dry ice/brine bath. Trimethylchlorosilane (1.0 mL; 8.28 mmol) was added dropwise over several minutes. Once the addition was complete, the reaction was stirred for 20 min, after which time, the reaction was removed from the bath. Upon standing for 20 min, a white powder precipitated, and the reaction was stirred at room temperature for a further 18 h. The mixture was filtered through Celite, and the filtrate was concentrated under reduced pressure to dryness. The crude product was heated to 110 °C for 15 min and then taken up in pentane (30 mL). X-ray quality crystals were grown from saturated solutions in toluene at ca. −20 °C over several weeks. Yield: 2.8 g (80%). Anal. Calcd. for $C_{30}H_{39}Al$: C, 84.46; H, 9.21. Found: C, 85.01; H, 9.08. ^1H NMR (300 MHz, C_6D_6, 25 °C): δ 7.303 (t, 2H *J* = 7.8 Hz) 7.150 (t, 1H *J* = 7.5 Hz) 7.057 (d, 4H *J* = 7.5 Hz) 7.004 (d, 2H *J* = 7.8 Hz) 2.767 (sept, 4H *J* = 6.9 Hz) 2.383 (bs, 2H) 1.042 (d, 12H *J* = 6.9 Hz) 1.000 (d, 12H *J* = 6.9 Hz). ^{13}C NMR (75 MHz, C_6D_6, 25 °C): δ 137.58, 128.53, 128.20, 127.55, 127.25, 105.00, 36.64, 36.00, 35.90. FTIR (cm^{-1}): 1906 m, 1934 m. mp 178 °C (with decomposition).

$(LiH_3AlAr^{iPr_8})_2$. $Ar^{iPr_8}Li(OEt_2)$ (5.01 g, 7.74 mmol) was dissolved in pentane (25 mL) and added dropwise to a rapidly stirred slurry of $AlH_3{\cdot}NMe_3$ (0.696 g, 7.81 mmol) in pentane (25 mL) at ca. 0 °C. After stirring for 30 min, the ice bath was removed, and the reaction was stirred at room temperature for 16 h. The precipitate was filtered off, and the filtrate was concentrated under reduced pressure to afford **1** as a white powder, which was essentially pure by ^1H NMR spectroscopy. Yield: 3.75 g (72%). Anal. Calcd. for $C_{36}H_{66}AlLi$: C, 81.15; H, 12.49. Found: C, 80.92; H, 12.41. ^1H NMR (300 MHz, C_6D_6, 25 °C): δ 7.54 (s, 1H *p*-*H*-C_6-2,6-Trip), 7.20 (s, 4H *m*-*H*-Trip), 2.96 (m, 6H $(CH_3)_2CH$(Trip)), 2.66 (sept *J* = 6.6 Hz, 2H $(CH_3)_2CH$(Ph)), 2.21 (broad s, 1H Al-*H*), 2.00 (broad s, 2H Al-*H*), 1.39 (d *J* = 6.7 Hz, 12H *m*-$(CH_3)_2CH$(Ph)), 1.33 (d *J* = 6.9 Hz, 12H *p*-$(CH_3)_2CH$(Trip)), 1.184 (d *J* = 6.7 Hz, 12H *o*-$(CH_3)_2CH$-(Trip)) 1.12 (d, *J* = 6.7 12H *o*-$(CH_3)_2CH$(Trip)). ^{13}C NMR (126 MHz, C_6D_6, 25 °C): δ 149.38, 148.12, 147.87, 145.56, 144.33, 141.58, 128.68, 128.50, 128.31, 122.82, 121.37, 121.13, 35.14, 34.33, 31.04, 30.46, 30.27, 26.51, 25.84, 25.74, 25.41, 24.98, 24.78, 24.49. FTIR, cm^{-1} ν(Al−H) = 1864 str, 1684 m. mp 128 °C (with decomposition).

$(Ar^{iPr_8}AlH_2)_2$. $(LiH_3AlAr^{iPr_8})_2$ (3.75 g, 5.59 mmol) was dissolved in pentane (25 mL) and cooled to 0 °C. Me_3SiCl (0.7 mL, 5.51 mmol) was added slowly over several minutes, and the reaction was allowed to warm to room temperature. After ca. 10 min, solid LiCl precipitated and stirring was continued overnight. The solids were allowed to settle, the reaction was filtered, and the filtrate was concentrated to dryness. Yield 2.0 g (60.1%). ^1H NMR (300 MHz, C_6D_6, 25 °C): δ 7.47 (s 1H), 7.14 (s 4H), 2.93 (sept *J* = 6.8 Hz, 2H), 2.74 (sept *J* = 6.7 Hz, 4H), 2.54 (sept *J* = 6.7 Hz, 2H) 2.47 (broad s ∼1H), 1.36 (d *J* = 6.9 Hz, 12H), 1.21 (d *J* = 6.8 Hz, 12H), 1.17 (d *J* = 6.8, 12H), 1.09 (d *J* = 6.7 Hz, 12H). ^{13}C NMR (75 MHz, C_6D_6, 25 °C): δ 171.70, 146.30, 145.73, 144.77, 143.61, 136.62, 123.19, 120.51, 32.75, 29.08, 28.34, 25.09, 24.35, 23.93, 22.87. FTIR: cm^{-1} ν(Al−H) 1934 m, 1909 m. mp 165 °C (with decomposition).

Reactions with NH_3. In typical experiments, 0.150 g of $(Ar^{Me_6}AlH_2)_2$, $(Ar^{iPr_4}AlH_2)_2$, or $(Ar^{iPr_8}AlH_2)_2$ was dissolved in toluene (30 mL) and treated with 2 equiv of NH_3 gas. The reaction was stirred for 18 h, and the resulting colorless solution was concentrated under reduced pressure until precipitation was observed. The mixture was then warmed to redissolve the precipitate and stored at ca. −20 °C for several days. This afforded crystalline material for all products, but only those of $\{Ar^{iPr_4}Al(H)NH_2\}_2$ (**1**) and $\{Ar^{iPr_8}Al(H)NH_2\}_2$ (**2**) produced crystals suitable for single crystal X-ray diffraction.

$\{Ar^{Me_6}AlH(NH_2)\}_2$ (1). ^1H NMR (25 °C, C_6D_6 300 MHz): δ −0.44 (s, 2H NH_2), 1.99 (s, 12H *o*-$C_6H_2(CH_3)_2$), 2.23 (s, 6H *p*-$C_6H_2(CH_3)$), 3.56 (bs, 1H Al-*H*), 6.77 (s, 4H $C_6H_2(CH_3)_2$), 6.87 (d, 2H *m*-$C_6H_3Mes_2$ $^3J_{HH}$ = 7.56 Hz), 7.22 (t, 1H *p*-$C_6H_3Mes_2$ $^3J_{HH}$ = 7.65 Hz). FTIR (cm^{-1}): 1900, 1868 (w), 1600 (m). mp 188 °C (with decomposition).

$\{Ar^{iPr_4}AlH(NH_2)\}_2$ (2). ^1H NMR (25 °C, C_6D_6 300 MHz): δ −0.68 (s, 2H NH_2), 1.05 (d, 12H,$(CH_3)_2C$), $^3J_{HH}$ = 5.1 Hz), 1.20 (d, 12H, $(CH_3)_2C$), $^3J_{HH}$ = 5.16 Hz), 2.88 (sept, 4H $(CH_3)_2CH$, $^3J_{HH}$ = 4.92 Hz), 7.09 (d, 4H *m*-C_6H_2 $^3J_{HH}$ = 2.34 Hz), 7.10 (d, 4H *m*-C_6H_2 $^3J_{HH}$ =

dx.doi.org/10.1021/om4010675 | *Organometallics* 2014, 33, 329−337

2.34 Hz), 7.23−7.27 (m, 3H, *p*-C_6H). FTIR (cm^{-1}): 1895 w, 1860 w, 1603 m. mp 172 °C (with decomposition). Yield: 0.2 g (66%).

{Ar^{iPrs}AlH(NH$_2$)}$_2$ (3). ^{1}H NMR (25 °C, C_6D_6 300 MHz): δ −0.22 (s, 2H NH_2), 1.18 (d, 12H $(CH_3)_2C$ $^3J_{HH}$ =6.66 Hz), 1.19 (d, 12H $(CH_3)_2C$ $^3J_{HH}$ =6.75 Hz), 1.27 (d, 12H $(CH_3)_2C$ $^3J_{HH}$ =6.78 Hz), 1.38 (d, 12H $(CH_3)_2C$ $^3J_{HH}$ = 6.90 Hz), 2.62 (sept, 2H $(CH_3)_2CH$ $^3J_{HH}$ = 6.66 Hz), 2.80 - 3.00 (m, 7H $(CH_3)_2CH$ and Al-*H*), 7.15 (s, 4H *m*-C_6H_2), 7.49 (s, 4H *p*-C_6HAr_2). FTIR (KBr press) cm^{-1}: 3365 m, 3354 m, 3332 m, 3299 m, 2965 s, 2868 m, 1899 m, 1870 m. mp 170 °C (with decomposition).

Reaction of (Ar^{Me_6}AlH$_2$)$_2$ with PH$_3$. In a typical experiment, 0.15 g of $(Ar^{Me_6}AlH_2)_2$ were dissolved in 12 mL of toluene in a stainless steel Parr reactor. Gaseous PH_3 was introduced to the vessel at a pressure of 80 psi. The solution was stirred for 24 h, after which the remaining PH_3 was swept out of the reactor with nitrogen and burnt. The solvent was removed under reduced pressure to afford a colorless solid. Recrystallization of the solid from pentane at −35 °C provided X-ray quality crystals of $\{(Ar^{Me_6}Al)_3(\mu\text{-}PH_2)_3(\mu\text{-}PH)(PH_2)\}$ (**4**). The solvent had to be removed quickly, as the compound would redissolve as the temperature increased, and the unit cell also had solvent molecules present.

{(Ar^{Me_6}Al)$_3$(μ-PH$_2$)$_3$(μ-PH)(PH$_2$)} (4). ^{1}H NMR (25 °C, C_6D_6, 400 MHz Varian INOVA): δ −1.16 (dt, 1H P*H*, $^1J_{PH}$ = 169 Hz, $^4J_{HH}$ = 20.5 Hz), −0.22 (dt, 2H PH_2, $^1J_{PH}$ = 178 Hz, $^4J_{HH}$ = 8.1 Hz), 0.85−1.50 (6H, PH_2 overlapped by pentane from crystal lattice) 2.024−2.120 (5 overlapping singlets, 42H *o*-$C_6H_2(CH_3)_2$), 2.279−2.291 (s, 12H *p*-$C_6H_2(CH_3)$), 6.775−6.979 (m, 18H $C_6H_2(CH_3)_2$ and *m*-$C_6H_3Mes_2$), 7.192−7.285 (3 overlapping triplets, 3H); $^{13}C\{^1H\}$ (25 °C, C_6D_6, 100.5 MHz Varian INOVA): δ 21.00, 21.53, 21.77, 21.80, 21.95, 22.04, 127.44, 127.72, 128.72, 129.14, 129.21, 129.44, 129.59, 129.69, 135.91, 136.57, 136.60, 136.70, 137.03, 137.05, 142.24, 142.53, 150.67, 151.08. $^{31}P\{^1H\}$ NMR (25 °C, C_6D_6, 161.8 MHz Varian INOVA): A_2BCD spin system, δ −264.6 (P_c, 1P, td, $^2J_{Pa\text{-}Pc}$ = 82.5 Hz, $^2J_{Pc\text{-}Pd}$ = 27.5 Hz), −257.9 (P_b, 1P, td, $^2J_{Pa-Pb}$ = 26.7 Hz, $^4J_{Pb-Pd}$ = 17.2 Hz), −200.6 (P_a, 2P, td, $^2J_{Pa-Pb}$ = 26.7 Hz, $^2J_{Pa\text{-}Pc}$ = 82.5 Hz, $^2J_{Pa-Pd}$ = 62.2 Hz), −182.0 (P_d, 1P, tdd, $^2J_{Pa-Pd}$ = 62.2 Hz, $^2J_{Pc\text{-}Pd}$ = 27.5 Hz, $^4J_{Pb-Pd}$ = 17.2 Hz). ^{31}P NMR (C_6D_6): δ −264.6 (dt, $^1J_{P-H}$ = 168 Hz, $^2J_{P-P}$ = 82.5 Hz), −257.9 (tq, $^1J_{P-H}$ = 175 Hz, $^3J_{P-H}$ = 19.0 Hz), −200.6 (t, $^1J_{P-H}$ = 299 Hz), −182.0 (t, $^1J_{P-H}$ = 295 Hz). FTIR (KBr, cm^{-1}): 444, 475, 558, 644, 737, 805, 848, 876, 921, 972, 1030, 1079, 1107, 1173, 1221, 1255, 1375, 1440, 1481, 1551, 1609, 2283, 2346, 2729, 2854, 2914, 2944, 3027.

{(Ar^{Me_6}Al)$_4$(PH$_2$)$_4$(PH)$_2$} (5). Single crystals of $\{(Ar^{Me_6}Al)_4(PH_2)_4(PH)_2\}$ suitable for diffraction experiments were reproducibly obtained by vapor diffusion of a pentane solution of the crude product into hexane. Quantities of **5** of suitable purity for full characterization could not be obtained because of the small percentage formed in the reaction. $^{31}P\{^1H\}$ NMR (25 °C, C_6D_6, 161.8 MHz Varian INOVA): δ −272.3 (t, 2P, *P*H, $^2J_{P-P}$ = 25 Hz), −207 (broad triplet, 4P, *P*H_2, $^2J_{P-P}$ = 25 Hz). ^{31}P NMR (C_6D_6): δ −272.3 (d, *P*H, $^1J_{P-H}$ = 168 Hz), −207 (t, *P*H_2, $^1J_{P-H}$ = 290 Hz).

X-ray Crystallographic Data Collection. X-ray quality crystals of **2**−**5** were covered with a layer of hydrocarbon oil. A suitable crystal was selected, attached to a glass fiber, and placed in the cold temperature stream.[48] For **2** and **3**, the data were collected at 90 K using a Nonius KappaCCD area detector or a Bruker Apex II Duo diffractometer using Mo Kα (λ = 0.71073 Å) or Cu Kα (λ = 1.54178 Å) radiation. For **4** and **5**, crystals were mounted on a MiTeGen polyimide micromount, and collected at 110 K on a Bruker Apex II detector using Mo Kα radiation (λ = 0.71073 Å). Absorption corrections were applied using SADABS.[49] The structures were solved by use of direct methods in SHELXS[50] and refined by the full-matrix least-squares procedure in SHELXL.[50] All non-hydrogen atoms were refined anisotropically, while carbon hydrogen atoms were placed at calculated positions and included in the refinement by using a riding model. The nitrogen, phosphorus, and aluminum hydrogens were located on a difference map and refined. Further details are given in Table S12 (Supporting Information). Several special refining details for compounds **4** and **5** should be described, with further details being found in the CIF file part of the Supporting Information. For compound **4** residual electron density consistent with 8 pentane molecules (2 per asymmetric unit) was present in the unit cell. These molecules were disordered and could not be modeled satisfactorily despite the use of restraints. It is also possible that these molecules were disordered benzene or toluene solvates, further adding to the potential disorder. As a result this electron density was treated as a diffuse contribution to the overall scattering by the SQUEEZE/platon program.[51] For compound **5** there are two toluene molecules in the asymmetric unit that are disordered. Any attempts to model this disorder were met with failure. However the molecules could be restrained to sensible parameters by the use of SIMU, DELU, and DFIX. The .res file is attached to the end of the .cif file for further details. Furthermore there were four pentane molecules in the unit cell, consistent with one full pentane molecule per asymmetric unit. These existed as two fragments with half a pentane in the asymmetric unit that exist on special positions by which the other half of the solvent molecules could be grown. These fragments were disordered and any attempted modeling or the use of restraints was unsuccessful. As a result this solvate was treated as a diffuse contribution to the overall scattering by the SQUEEZE/platon program.

■ ASSOCIATED CONTENT

Ⓢ Supporting Information

CIF files for **2**−**5**, 1H NMR spectra of $(H_2AlAr^{Pr^i}{}_4)_2$, $(H_2AlAr^{Pr^i}{}_8)_2$, $LiH_3AlAr^{Pr^i}{}_4$, $LiH_3AlAr^{Pr^i}{}_8$, and **1**−**3**, ^1H and ^{31}P NMR spectra of **4** and **5**, and a drawing illustrating the disordered core structure of **4**. This material is available free of charge via the Internet at http://pubs.acs.org.

■ AUTHOR INFORMATION

Corresponding Author

*E-mail: pppower@ucdavis.edu.

Notes

The authors declare no competing financial interest.

■ ACKNOWLEDGMENTS

We thank the U.S. Department of Energy (DE-FG02-07ER46475), the Natural Science and Engineering Research Counsel (NSERC), the Ontario government, the Canadian Foundation for Innovation (CFI), and The Unverisity of Western Ontario for financial support. The phosphine experiments were aided by the support of Cytec industries and the brilliance of the chemistry department electronic shop (J. Vanstone and J. Aukema).

■ REFERENCES

(1) Janik, J. F.; Duesler, E. N.; Paine, R. T. *Inorg. Chem.* **1987**, *26*, 4341−4344.

(2) Paciorek, K.; Nakahara, J. H.; Hoferkamp, L. A.; George, C.; Flippen-Anderson, J. L.; Gilardi, R.; Schmidt, W. R. *Chem. Mater.* **1991**, *3*, 82−87.

(3) Janik, J. F.; Duesler, E. N.; Paine, R. T. *Inorg. Chem.* **1988**, *27*, 4335−4338.

(4) Interrante, L. V.; Sigel, G. A.; Garbauskas, M.; Hejna, C.; Slack, G. A. *Inorg. Chem.* **2001**, *28*, 252−257.

(5) Jancik, V.; Pineda, L. W.; Pinkas, J.; Roesky, H. W.; Neculai, D.; Neculai, A. M.; Herbst-Irmer, R. *Angew. Chem., Int. Ed. Engl.* **2004**, *43*, 2142−2145.

(6) *The Group 13 Metals Aluminium, Gallium, Indium, and Thallium: Chemical Patterns and Peculiarities*; Aldridge, S., Downs, A. J., Eds.; Wiley: Chichester, 2011.

(7) Lappert, M. F.; Power, P. P.; Protchenko, A.; Seeber, A. *Metal Amide Chemistry*; Wiley: Chichester, 2009.

(8) Finholt, A. E.; Helling, C.; Imhof, V.; Nielsen, L.; Jacobson, E. *Inorg. Chem.* **1963**, *2*, 504−507.
(9) Baudler, M.; Scholz, G.; Tebbe, K.-F. *Z. Anorg. Allg. Chem.* **1990**, *581*, 111−124.
(10) von Hänisch, C. *Eur. J. Inorg. Chem.* **2003**, 2955−2958.
(11) Driess, M.; Monsé, C. *Z. Anorg. Allg. Chem.* **2000**, *626*, 1091−1094.
(12) Vogel, U.; Timoshkin, A. Y.; Scheer, M. *Angew. Chem., Int. Ed. Engl.* **2001**, *40*, 4409−4412.
(13) Vogel, U.; Schwan, K.-C.; Scheer, M. *Eur. J. Inorg. Chem.* **2004**, *2004*, 2062−2065.
(14) Vogel, U.; Timoshkin, A. Y.; Schwan, K.-C.; Bodensteiner, M.; Scheer, M. *J. Organomet. Chem.* **2006**, *691*, 4556−4564.
(15) (a) Bodensteiner, M.; Vogel, U.; Timoshkin, A. Y.; Scheer, M. *Angew. Chem., Int. Ed. Engl.* **2009**, *48*, 4629−4633. (b) Bodensteiner, M.; Timoshkin, A. Y.; Peresypkina, E. V.; Vogel, U.; Scheer, M. *Chem.—Eur. J.* **2013**, *19*, 957−963.
(16) Wehmschulte, R. J.; Grigsby, W. J.; Schiemenz, B.; Bartlett, R. A.; Power, P. P. *Inorg. Chem.* **1996**, *35*, 6694−6702.
(17) Zhu, Z.; Wang, X.; Peng, Y.; Lei, H.; Fettinger, J. C.; Rivard, E.; Power, P. P. *Angew. Chem., Int. Ed. Engl.* **2009**, *48*, 2031−2034.
(18) Coates, G. E. *J. Chem. Soc.* **1951**, 2003−2013.
(19) Hwang, J.-W.; Hanson, S. A.; Britton, J. F.; Evans, K. F.; Jensen, K. F.; Gladfelter, W. L. *Chem. Mater.* **1990**, *2*, 342−343.
(20) Almond, M. J.; Drew, M. G. B.; Jenkins, C. E.; Rice, D. A. J. *J. Chem. Soc., Dalton Trans.* **1992**, 5−9.
(21) Park, H. S.; Waezsada, S. D.; Cowley, A. H.; Roesky, H. W. *Chem. Mater.* **1998**, *10*, 2251−2257.
(22) Beachley, O. T.; Pazik, J. C.; Noble, M. J. *Organometallics* **1998**, *17*, 2121−2123.
(23) Atwood, D. A.; Cowley, A. H.; Harris, P. R.; Jones, R. A.; Koschmieder, S. U.; Nunn, C. M.; Atwood, J. L.; Bolt, S. G. *Organometallics* **1993**, *12*, 24−29.
(24) Jancik, V.; Pineda, L. W.; Stücke, A. C.; Roesky, H. W.; Herbst-Irmer, R. *Organometallics* **2005**, *24*, 1511−1515.
(25) Coates, G. E.; Graham, J. *J. Chem. Soc.* **1963**, 223−228.
(26) Beachley, O. T.; Coates, G. E. *J. Chem. Soc.* **1965**, 3241−3247.
(27) Cowley, A. H.; Harris, P. R.; Jones, R. A.; Nunn, C. M. *Organometallics* **1991**, *10*, 652−656.
(28) Li, X.-W.; Wei, P.; Beck, B. C.; Xie, Y.; Schaefer, H. F., III; Su, J.; Robinson, G. H. *Chem. Commun.* **2000**, 453−454.
(29) Pytlewski, L. L.; Nixon, E. R. *Inorg. Chem.* **1963**, *2*, 763−764.
(30) Pytlewski, L. L.; Howell, J. K. *Chem. Commun.* **1967**, 1280.
(31) Howell, J. K.; Pytlewski, L. L. *Inorg. Nucl. Chem. Lett.* **1970**, *6*, 681−686.
(32) Dou, D.; Linti, G. W.; Chen, T.; Duesler, E. N.; Paine, R. T.; Nöth, H. *Inorg. Chem.* **1996**, *35*, 3626−3634.
(33) *Tables of Interatomic Distances and Configurations in Molecules and Ions*; Sutton, L., Ed.; The Chemical Society: London, 1958 and 1965; Spec. Publ. Nos. 11 and 18.
(34) (a) Schomaker, V.; Stevenson, D. P. *J. Am. Chem. Soc.* **1941**, *63*, 37−41. (b) Brothers, P. J.; Power, P. P. *Adv. Organomet. Chem.* **1996**, *39*, 1−70.
(35) Wehmschulte, R. J.; Power, P. P. *Inorg. Chem.* **1996**, *35*, 3262−3267.
(36) Wells, R. L.; Rahbarnoohi, H.; Glaser, P. B.; Liable-Sands, L. M.; Rheingold, A. L. *Organometallics* **1996**, *15*, 3204−3209.
(37) Janik, J. F.; Duesler, E. N.; McNamara, W. F.; Westerhausen, M.; Paine, R. T. *Organometallics* **1989**, *8*, 506−514.
(38) Amoureux, J. P.; Bee, M.; Damien, J. C. *Acta Crystallogr., Sect. B: Struct. Crystallogr. Cryst. Chem.* **1980**, *36*, 2633−2636.
(39) Boardman, A.; Jeffs, S. E.; Small, R. W. H.; Worrall, I. J. *Inorg. Chim. Acta* **1984**, *83*, L39−L40.
(40) Boardman, A.; Small, R. W. H.; Worrall, I. J. *Inorg. Chim. Acta* **1986**, *120*, L23−L24.
(41) Schnitter, C.; Roesky, H. W.; Albers, T.; Schmidt, H.-G.; Röpken, C.; Parisini, E.; Sheldrick, G. M. *Chem.—Eur. J.* **1997**, *3*, 1783−1792.
(42) Luo, B.; Gladfelter, W. L. *Inorg. Chem.* **2002**, *41*, 6249−6257.
(43) Young, J. D.; Khan, M. A.; Powell, D. R.; Wehmschulte, R. J. *Eur. J. Inorg. Chem.* **2007**, *2007*, 1671−1681.
(44) Pangborn, A. B.; Giardello, M. A.; Grubbs, R. H.; Rosen, R. K.; Timmers, F. J. *Organometallics* **1996**, *15*, 1518−1520.
(45) Kovar, R. A.; Callaway, J. O. *Inorg. Synth.* **1977**, *17*, 36−39.
(46) Schiemenz, B.; Power, P. P. *Angew. Chem., Int. Ed.* **1996**, *35*, 2150−2152.
(47) Stanciu, C.; Richards, A. F.; Fettinger, J. C.; Brynda, M.; Power, P. P. *J. Organomet. Chem.* **2006**, *691*, 2540−2545.
(48) Hope, H. *Prog. Inorg. Chem.* **1995**, *41*, 1−19.
(49) *SADABS: Area Detection Absorption Correction*; Bruker AXS, Inc.: Madison, WI, 1996.
(50) *SHELXS and SHELXL*, Version 5.03; Bruker AXS, Inc.: Madison, WI, 1994.
(51) van der Sluis, P.; Spek, A. L. *Acta Crystallogr., Sect. A: Found. Crystallogr.* **1990**, *46*, 194−201.